

On the effective Dirac dynamics of ultracold atoms in bichromatic optical lattices

D. Witthaut

Max-Planck-Institute for Dynamics and Self-Organization, D-37073 Göttingen, Germany

T. Salger, S. Kling, C. Grossert, and M. Weitz

Institut für Angewandte Physik, Universität Bonn, D-53115 Bonn, Germany

(Dated: January 12, 2013)

We study the dynamics of ultracold atoms in tailored bichromatic optical lattices. By tuning the lattice parameters, one can readily engineer the band structure and realize a Dirac point, i.e. a true crossing of two Bloch bands. The dynamics in the vicinity of such a crossing is described by the one-dimensional Dirac equation, which is rigorously shown beyond the tight-binding approximation. Within this framework we analyze the effects of an external potential and demonstrate numerically that it is possible to demonstrate Klein tunneling with current experimental setups.

PACS numbers: 03.75.Mn, 03.67.Ac, 03.65.Pm

I. INTRODUCTION

Quantum simulators aim at the simulation of complex quantum systems in well controllable laboratory experiments [1]. Such a simulation is especially useful when the original quantum system is experimentally not accessible and numerical simulations are impossible due to the exponential size of the Hilbert space. Furthermore, quantum simulators offer the possibility to tune the experimental parameters to explore novel physical phenomena. Important examples include the simulation of solid state systems with ultracold atoms [2], sonic black holes in Bose-Einstein condensates [3] and the Dirac dynamics with trapped ions [4–7].

Ultracold atoms in optical lattices are especially suited for such a task, since their dynamics can be controlled with an astonishing precision and their dynamics can be measured in situ. Bichromatic lattices are especially appealing since these systems allow to tune the energy dispersion of the Bloch bands. In particular one can choose the parameters such that a Dirac point, i.e. a true crossing of the first and second excited band, is realized depending on the relative phase between the two fundamental lattices. Unlike other systems [8–10], bichromatic optical lattices thus allow to simulate relativistic quantum effects using only a single species of neutral atoms and no external driving fields. This approach therefore paves the way for the simulation of interacting relativistic quantum field theories [11].

In this paper we investigate the dynamics around a Dirac point in detail and derive the one-dimensional Dirac equation as an effective equation of motion for the coarse-grained atomic wave functions. In contrast to previous approaches [11–14], we do *not* make use of a tight-binding approximation, such that the Dirac equation is found without imposing a continuum limit. We discuss the effects of an external potential in detail, showing that the Dirac description remains valid if the potential varies slowly enough. Within this framework we finally show that it is possible to simulate Klein tunneling through a potential barrier with current experimental methods.

II. BLOCH AND WANNIER STATES IN BICHROMATIC OPTICAL LATTICES

We consider the dynamics of ultracold atoms in a bichromatic optical lattice described by the Hamiltonian

$$\hat{H}_0 = \frac{-\hbar^2}{2M} \frac{\partial^2}{\partial x^2} + \frac{V_1}{2} \cos(2k_0 x) + \frac{V_2}{2} \cos(4k_0 x + \phi) \quad (1)$$

plus an additional potential $V(x)$, which is assumed to vary slowly compared to $k_0 x$. A bichromatic optical lattice with arbitrary relative phase ϕ can be implemented by a superposition of an ordinary optical lattice with a periodicity of $\lambda/2$ and an additional lattice with a periodicity of $\lambda/4$ based on four-photon processes as described in [15–17]. For the additional potential $V(x)$ we consider (i) an optical dipole trap and (ii) a static field which can be realized by either gravity or accelerating the complete lattice. In the following we will use scaled units which are obtained by setting $x' = k_0 x$, $t' = E_R t / \hbar$ and dividing the Schrödinger equation by the recoil energy $E_R = \hbar^2 k_0^2 / 2M$. In these units we have $\hbar = 1$ and $M = 1/2$ and all energies are given in units of E_R .

The eigenstates of \hat{H}_0 , the Bloch waves can be engineered to a large extent by choosing the lattice parameters $V_{1,2}$ and ϕ which makes bichromatic lattices a convenient tool for quantum simulations. To be precise, the Bloch states are defined as the simultaneous eigenstates of \hat{H}_0 and the translation T_d over the lattice period d :

$$\begin{aligned} \hat{H}_0 u_{\alpha, \kappa}(x) &= E_{\alpha}(\kappa) u_{\alpha, \kappa}(x), \\ T_d u_{\alpha, \kappa}(x) &= e^{id\kappa} u_{\alpha, \kappa}(x). \end{aligned} \quad (2)$$

Here and in the following, $\kappa \in [-\pi/d, \pi/d]$ is the quasi momentum and $\alpha = 0, 1, 2, \dots$ labels the different Bloch bands. Figure 1 shows the bandstructure $E_{\alpha}(\kappa)$ of a bichromatic lattice with $V_1 = 5$ and $V_2 = 1.56$, comparing two different choices of the relative phase ϕ . For these values of the lattice depth and a relative phase $\phi = \pi$, one observes a true crossing of the eigenenergies of the first and second excited band at $\kappa = 0$, i.e. a so-called

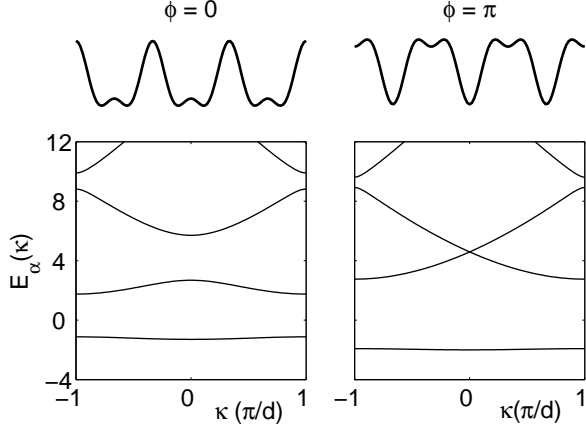


FIG. 1: The lowest Bloch bands for the case $V_1 = 5$ and $V_2 = 1.56$. For $\phi = \pi$ one observes a true crossing between the first and the second excited band, a Dirac point, which can be used to simulate the Dirac equation.

'Dirac point'. The physical reason for the vanishing of the band gap is that the contributions of the second order Bragg scattering at the optical lattice with periodicity $\lambda/2$ and the first order Bragg scattering at the lattice with periodicity $\lambda/4$ show a complete destructive interference for the given parameters. At the Dirac point the dispersion relation is linear in κ , just as for a relativistic massless Dirac particle, such that a similar dynamics can be expected. We will make this analogy more precise in the following. In general, the band gap between the first and second excited band is approximately given by $\Delta E \approx |(V_1/4)^2 + V_2 \exp(i\phi)|$ [16].

However, also for a small but finite band gap we obtain a pseudo-relativistic dynamics in the center of the Brillouin zone. In any case, we can approximate the energy dispersion of the first and second excited band around $\kappa \approx 0$ as

$$E_{1,2}(\kappa) = E_D \pm \sqrt{m^2 c^4 + c^2 \kappa^2}. \quad (3)$$

This relation defines an effective mass m which is given by the curvature of the two bands and an effective speed of light c which is related to the band gap by

$$\Delta E = 2mc^2. \quad (4)$$

The applicability of this approximation is illustrated in Fig. 2, where it is compared to the numerically exact data. Furthermore, the figure shows the effective parameters m and c as a function of the lattice phase ϕ .

Now it is very convenient to introduce a new basis in which the two Bloch states in the first and second excited band are rotated:

$$\begin{aligned} \tilde{u}_{1,\kappa} &= \cos \theta u_{1,\kappa} + \sin \theta u_{2,\kappa} \\ \tilde{u}_{2,\kappa} &= -\sin \theta u_{1,\kappa} + \cos \theta u_{2,\kappa} \end{aligned} \quad (5)$$

with the mixing angle

$$\tan \theta(\kappa) = \frac{mc^2}{c\kappa + \sqrt{m^2 c^4 + c^2 \kappa^2}}. \quad (6)$$

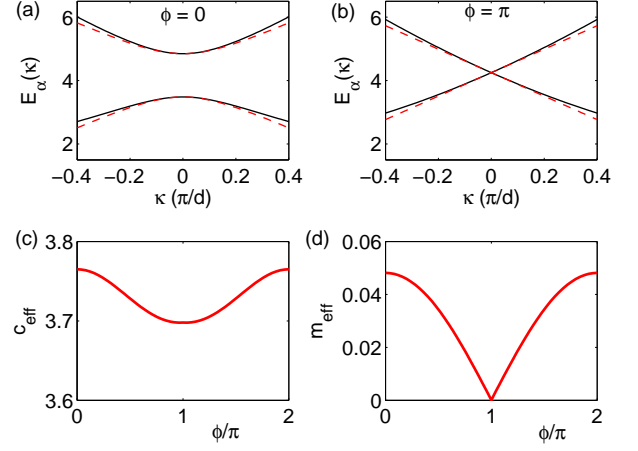


FIG. 2: (Color online) (a,b) A fit of the relativistic dispersion relation (3) to the Bloch bands $\alpha = 1, 2$ in the center of the Brillouin zone for $\phi = 0$ and $\phi = \pi$, respectively. (c,d) The resulting fit values for the effective parameters m and c as a function of the phase ϕ . The remaining parameters are the same as in Fig. 1.

In this basis, the free Hamiltonian \hat{H}_0 is no longer diagonal, but has the convenient form

$$\hat{H}_0(\kappa) = \begin{pmatrix} E_D + c\kappa & mc^2 \\ mc^2 & E_D - c\kappa \end{pmatrix} \quad (7)$$

The eigenenergies (3) for given quasimomentum κ are simply the eigenvalues of the matrix $\hat{H}_0(\kappa)$.

For an effective description of the quantum dynamics in a perturbed crystal we will furthermore need the Wannier basis which is defined as follows. The Bloch waves can be chosen to be periodic in the quasi momentum κ , such that they can be expanded into a Fourier series,

$$u_{\alpha,\kappa}(x) = \frac{d}{\sqrt{2\pi}} \sum_{n \in \mathbb{Z}} e^{i\kappa d n} w_{\alpha,n}(x), \quad (8)$$

which defines the Wannier states $w_{\alpha,n}(x)$. Inverting the Fourier series yields

$$w_{\alpha,n}(x) = \frac{1}{\sqrt{2\pi d}} \int e^{-i\kappa d n} u_{\alpha,\kappa}(x) d\kappa. \quad (9)$$

The Wannier states are exponentially localized at the lattice site n [19], and they are related by a simple shift in real space

$$w_{\alpha,n}(x) = w_{\alpha,0}(x - x_n), \quad (10)$$

where $x_n = nd$ is the position of the n th lattice well. These properties are quite useful for several approximation schemes (cf. [20]). Examples for the case of a bichromatic lattice are shown in Fig. 3 for two values of the relative phase ϕ .

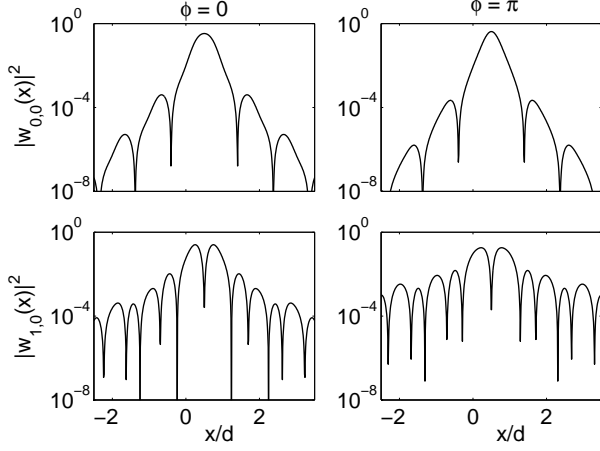


FIG. 3: Squared modulus of the Wannier states $|w_{\alpha,n}(x)|^2$ in the ground ($\alpha = 0$, upper panels) and the first excited band ($\alpha = 1$, lower panels) at the lattice site $n = 0$ in a semi-logarithmic scale. We assume a bichromatic optical lattice with $V_1 = 5$, $V_2 = 1.56$ and $\phi = 0$ (left) and $\phi = \pi$, respectively.

III. EFFECTIVE EVOLUTION EQUATIONS

For the derivation of the effective evolution equations we start from the Wannier representation of an arbitrary wave function,

$$\Psi(x) = \sum_{\alpha,n} \psi_{\alpha,n} w_{\alpha,0}(x - x_n) \quad (11)$$

The expansion coefficients $\psi_{\alpha,n}$ form an infinite, but countable set of complex number. For the following approximations, however, we define a continuous function $\psi_\alpha(x)$ for every Bloch band α such that

$$\psi_\alpha(x_n) = \psi_{\alpha,n}. \quad (12)$$

These functions can be viewed as a coarse grained version of the quantum state $\Psi(x)$ projected on the band α . Now one can derive effective evolution equations for these coarse grained wave functions.

One can show that every operator, which is diagonal in the quasi momentum κ , can be expressed in a very convenient way for the coarse grained wave functions $\psi_\alpha(x)$. So consider an operator which satisfies

$$\hat{O} u_{\alpha,\kappa} = \sum_{\beta} O_{\beta,\alpha}(\kappa) u_{\beta,\kappa} \quad (13)$$

where $u_{\alpha,\kappa}$ are the Bloch states defined above. Then this operator acts on the coarse grained wave function as

$$\hat{O} \psi_\alpha(x) = \sum_{\beta} O_{\beta,\alpha}(\hat{p}) \psi_\beta(x), \quad (14)$$

i.e. the quasi momentum κ is replaced by the momentum operator $\hat{p} = -i\partial_x$. To carry out this replacement one

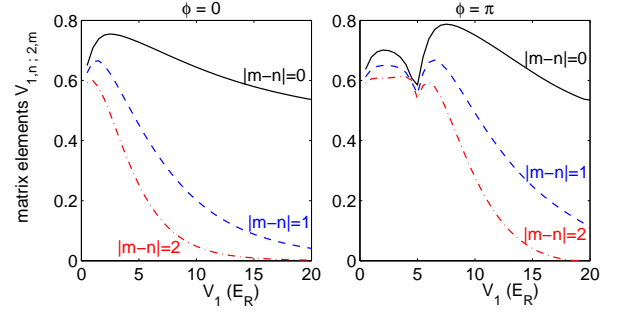


FIG. 4: (Color online) Matrix elements $V_{\alpha,n;\beta,m}$ of a linear potential $V(x) = x$ in a Wannier basis as a function of the lattice depth V_1 . We have plotted the matrix elements for $\alpha = 1$, $\beta = 2$ and $|n - m| \leq 2$, which are the leading corrections to the diagonal approximation (19). As above, we assume $V_2/V_1 = 1.56/5$ and $\phi = 0$ (left) and $\phi = \pi$ (right), respectively.

can expand $O_{\beta,\alpha}(\kappa)$ in a Taylor series and then replace every term κ^n by $(-i\partial_x)^n$. This relation was first shown by Slater [22], cf. also [23–25]. The proof is summarized in the appendix.

In particular, this holds for the lattice Hamiltonian \hat{H}_0 , which is trivially diagonal in the Bloch basis. Going to the rotated basis defined in equation (5), the eigenvalue equation for the lattice Hamiltonian reads

$$\hat{H}_0 \begin{pmatrix} \tilde{u}_{1,\kappa} \\ \tilde{u}_{2,\kappa} \end{pmatrix} = \begin{pmatrix} E_D + c\kappa & mc^2 \\ mc^2 & E_D - c\kappa \end{pmatrix} \begin{pmatrix} \tilde{u}_{1,\kappa} \\ \tilde{u}_{2,\kappa} \end{pmatrix} \quad (15)$$

The constant energy offset E_D introduces a global phase shift only, which has no physical significance. By shifting the energy scale, we can set it to zero, $E_D = 0$.

Now if we express a general quantum state in the first and second excited band as

$$\Psi(x) = \sum_{\alpha=1,2;n} \psi_\alpha(x_n) \tilde{w}_{\alpha,n}(x), \quad (16)$$

where the rotated Wannier function $\tilde{w}_{\alpha,n}(x)$ are related to the original ones $w_{\alpha,n}(x)$ by the same rotation as the used in Eqn. (5), then Slater's theorem tells us that the lattice Hamiltonian acts onto the coarse grained wave functions $\psi_\alpha(x)$ as

$$\hat{H}_0 \begin{pmatrix} \psi_1(x) \\ \psi_2(x) \end{pmatrix} = \begin{pmatrix} +c\hat{p} & mc^2 \\ mc^2 & -c\hat{p} \end{pmatrix} \begin{pmatrix} \psi_1(x) \\ \psi_2(x) \end{pmatrix}, \quad (17)$$

where $\hat{p} = -i\partial_x$ is the momentum operator.

In addition we need to know how a slowly varying potential $V(x)$ acts onto the functions $\psi_\alpha(x)$. We recall that these functions have been defined as expansion coefficients in the Wannier basis, such that we need the matrix elements

$$V_{\beta,n;\alpha,m} = \int dx w_{\beta,0}^*(x - x_m) V(x) w_{\alpha,0}(x - x_n). \quad (18)$$

Using the strong localization of the Wannier states, one can set $V(x)$ to a constant over the localization length

in a first approximation. Because of the orthogonality of the Wannier states one thus finds

$$V_{\beta,n;\alpha,m} \approx V(x_n)\delta_{\beta,\alpha}\delta_{n,m}. \quad (19)$$

Let us analyze this approximation in more detail for the case of a linear potential $V(x) = Fx$. Then we have

$$V_{\beta,n;\alpha,m} = Fx_n\delta_{\beta,\alpha}\delta_{n,m} + F \int dx w_{\beta,m-n}^*(x) x w_{\alpha,0}(x),$$

where Eqn. (10) has been used to simplify the results. The first term in this expression corresponds to the diagonal approximation (19), while the remaining matrix elements can be interpreted as follows. The local terms, i.e. the terms with $n = m$, vanish exactly for $\alpha = \beta$ due to the parity of the Wannier functions. The term $\alpha = 1$ and $\beta = 2$ is the most important correction to the diagonal approximation (19). It couples the two bands and can thus be viewed as an additional contribution to the effective mass mc^2 in the effective wave equation (17). The nonlocal terms $n \neq m$ are also largest for $\alpha = 1$ and $\beta = 2$. However, they vanish exponentially with the lattice depth $V_{1,2}$ and the squared lattice period d^2 . These matrix elements are plotted as a function of the lattice depth in Fig. 4, assuming $V_2/V_1 = 1.56/5$ and $\phi = 0, \pi$ as above. Note that the lattice depth in scaled units is proportional to d^2 . One clearly sees how the non-local terms vanish exponentially in contrast to the local term $n = m$.

In the following we will confine ourselves to the first order approximation (19). For the ansatz (16), the potential thus acts as

$$V(x) \sum_{\alpha,n} \psi_{\alpha}(x_n) \tilde{w}_{\alpha,n}(x) \approx \sum_{\alpha,n} V(x_n) \psi_{\alpha}(x_n) \tilde{w}_{\alpha,n}(x).$$

In this approximation, we thus find the effective evolution equations for the coarse grained wave function:

$$i \frac{\partial}{\partial t} \begin{pmatrix} \psi_1 \\ \psi_2 \end{pmatrix} = \begin{pmatrix} V(x) + c\hat{p} & mc^2 \\ mc^2 & V(x) - c\hat{p} \end{pmatrix} \begin{pmatrix} \psi_1 \\ \psi_2 \end{pmatrix}. \quad (20)$$

If we rotate the 'spinor' wave function (ψ_1, ψ_2) once again by the unitary transformation

$$U = \frac{1}{\sqrt{2}} \begin{pmatrix} 1 & -1 \\ 1 & 1 \end{pmatrix}, \quad (21)$$

we finally obtain the Dirac equation in 1+1 dimensions with an external scalar potential,

$$i \frac{\partial}{\partial t} \begin{pmatrix} \psi_a \\ \psi_b \end{pmatrix} = \begin{pmatrix} V(x) - mc^2 & c\hat{p} \\ c\hat{p} & V(x) + mc^2 \end{pmatrix} \begin{pmatrix} \psi_a \\ \psi_b \end{pmatrix}. \quad (22)$$

Note that in this rotated frame ψ_a and ψ_b coincide with the amplitudes in the first and second excited band for $\kappa = 0$ – but only there. Otherwise one has to be very careful when interpreting the wave functions.

IV. QUANTUM SIMULATION OF KLEIN TUNNELING

As an example of the effective relativistic dynamics we consider the tunneling of a wavepacket out of a dipole trap in a tilted bichromatic lattice. In particular, the slowly varying potential is given by

$$V(x) = -V_0 \exp(-2x^2/W_0^2) - Fx \quad (23)$$

with $F = 0.076$, $V_0 = 19.77$ and $W_0 = 157$ in scaled units, which corresponds to typical experimental parameters [16, 17]. Initially, the wave packet is localized in the second excited band with quasi momentum $\kappa = 0.95$ with a gaussian envelope of width $\sigma = 17$.

The resulting dynamics of the atoms is shown in Fig. 5. The sketch on the left demonstrates the two different regimes realized for $\phi = 0$ (a1, b1) and $\phi = \pi$ (a3, b3). In the latter case a Dirac point emerges in the band structure, such that the atoms behave like massless relativistic particles. Unlike a massive Schrödinger particle such a Dirac particle can escape from the trap via *Klein tunneling*.

This expectation is confirmed by the numerical simulation of the atomic dynamics. The upper panels (a1-a3) of Fig. 5 show the evolution of the modulus of the atomic wave function $|\Psi(x, t)|$, calculated with the original Schrödinger equation in a bichromatic optical lattice. The effective Dirac dynamics according to Eqn. (20) is shown in the lower panels (b1-b3). The effective values of the mass m and the speed of light c are given by $mc^2 = 0.78$ (b1), $mc^2 = 0.24$ (b2), and $mc^2 = 0$ (b3), respectively. For the sake of a better visibility we have again plotted the modulus $|\psi_1(x, t)| + |\psi_2(x, t)|$. One observes that the essential features of the atomic dynamics are very well reproduced by the Dirac approximation. In particular, one observes the transition from a 'heavy' Schrödinger-like particle for $\phi = 0$ (a1, b1) to a 'relativistic' particle with vanishing effective mass for $\phi = \pi$ (a3, b3), which escapes from the dipole trap by Klein tunneling. For $\phi = 0.8\pi$ (a2, b2), partial tunneling is observed and the potential barrier acts as a matter wave beam splitter.

The most obvious difference of the Dirac approximation (20) to the underlying lattice dynamics is that the group velocity of the Dirac wave packet is limited to the effective speed of light c . After tunneling out of the dipole trap, the atoms are accelerated by the linear potential Fx , which is not observed in an effective relativistic description. This difference is due to the fact that the wave packet is not restricted to the center of the Brillouin zone for the given parameters, as it was assumed in the derivation of the effective Dirac equation. Instead, we have $\kappa_{\text{initial}} = 0.9$ and $|\kappa_{\text{final}}| \lesssim 1$ in the example shown in Fig. 5.

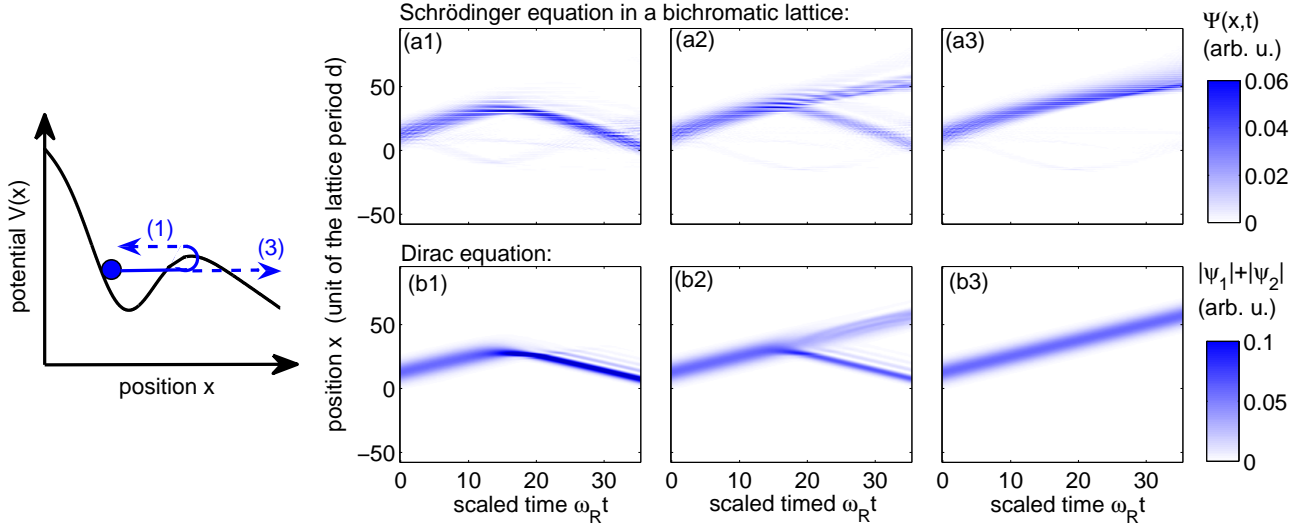


FIG. 5: (Color online) Quantum simulation of Klein-Tunneling out of a dipole trap. The upper panels (a1-a3) show the full time evolution of the Schrödinger equation in a bichromatic optical lattice for the case $V_1 = 5$ and $V_2 = 1.56$ and a relative phase of $\phi = 0$ (a1), $\phi = 0.8\pi$ (a2), and $\phi = \pi$ (a3). The lower panels (b1-b3) show the dynamics of the effective Dirac equation (20) with effective mass and speed of light given by $mc^2 = 0.78$ (b1), $mc^2 = 0.24$ (b2), and $mc^2 = 0$ (b3), respectively.

V. CONCLUSION AND OUTLOOK

We have analyzed the quantum dynamics of ultracold atoms in a bichromatic optical lattice. It was shown that the lattice parameters can be tuned such that a Dirac point emerges in the band structure, i.e. a true crossing of the Bloch bands with linear dispersion relation. In the vicinity of such a crossing the atoms effectively behave like massless relativistic particles, allowing for a tabletop simulation of relativistic quantum physics.

We have rigorously shown that the one-dimensional Dirac equation is found as an effective evolution equation for the coarse grained atomic wave function projected onto the two crossing Bloch bands. Unlike previous approaches, our derivation does not rely on a tight-binding approximation and also shows that how to include an additional, slowly varying potential. Therefore it is possible to simulate *Klein tunneling* – the tunneling of an ultrarelativistic particle through a potential barrier without damping – with current experimental setups.

Ultracold atoms in bichromatic optical lattices have some important advantages than other systems proposed before. The initial state of the atoms and all experimental parameters can be controlled with astonishing precision. In a common experiment, several thousands of ultracold atoms are prepared in the optical lattice. Thus it is possible to simulate the dynamics of *interacting* Dirac fermions in contrast to experiments with single trapped ions. While these experiments of course require the use of fermionic ultracold atoms, we note that Klein tunneling is a single particle effect such that it can be observed equally well for bosonic atoms.

Acknowledgments

We thank A. Rosch, H. Kroha and K. Ziegler for stimulating discussions. Financial support by the German Research Foundation (DFG) and the Max Planck society is gratefully acknowledged.

Appendix: Slater's derivation of the effective equation of motion

The wave function $\Psi(x, t)$ is expanded into Wannier states

$$\begin{aligned}\Psi(x, t) &= \sum_{\alpha, n} \psi_{\alpha, x} w_{\alpha, n}(x) \\ &= \sum_{\alpha, n} \psi_{\alpha}(x_n) w_{\alpha, 0}(x - x_n).\end{aligned}\quad (\text{A.1})$$

The wave function is thus represented by a discrete set of numbers $\psi_{\alpha, n}$. Due to the exponential localization of the Wannier states, these coefficients can be interpreted as the amplitude in the n th lattice site and in band α . For the effective evolution equations treat these coefficients as a continuous function in x , i.e. we choose a smooth function $\psi_{\alpha}(x)$ such that

$$\psi_{\alpha}(x_n) = \psi_{\alpha, n}.\quad (\text{A.2})$$

This function can be seen as a coarse grained version of the original wave function $\Psi(x)$ projected onto the α th Bloch band.

We consider an operator, which is diagonal in the quasi

momentum κ ,

$$\hat{O} u_{\alpha,\kappa} = \sum_{\beta} O_{\beta,\alpha}(\kappa) u_{\beta,\kappa}, \quad (\text{A.3})$$

as for instance the unperturbed Hamiltonian \hat{H}_0 . The functions $O_{\beta,\alpha}(\kappa)$ are periodic in κ , such that we can expand them into a Fourier series:

$$O_{\beta,\alpha}(\kappa) = \sum_s O_{\beta,\alpha}^{(s)} e^{-isd\kappa}. \quad (\text{A.4})$$

Applying this operator to a wave function of the form (A.1) and inserting the definition (9) for the Wannier function yields yields

$$\begin{aligned} \hat{O}\Psi(x) &= \sum_{\alpha,n} \psi_{\alpha}(x_n) \hat{O} w_{\alpha,n}(x) \\ &= \frac{1}{\sqrt{2\pi d}} \int d\kappa \sum_{\alpha,\beta,n,s} \psi_{\alpha}(x_n) O_{\beta,\alpha}^{(s)} e^{-i(n+s)d\kappa} u_{\beta,\kappa}(x). \end{aligned}$$

Using again equation (9) this can be rewritten as

$$\begin{aligned} \hat{O}\Psi(x) &= \sum_{\alpha,\beta,n,s} \psi_{\alpha}(x_n) O_{\beta,\alpha}^{(s)} w_{\beta}(x - x_{n+s}) \\ &= \sum_{\alpha,\beta,m,s} O_{\beta,\alpha}^{(s)} \psi_{\alpha}(x_m - x_s) w_{\beta}(x - x_m), \end{aligned}$$

where we have set $x_m = x_n + x_s$. Now one can use the the spatial translation operator and fact that we assumed $\psi_{\alpha}(x)$ to be a continuous function such that

$$\psi_{\alpha}(x_m - x_s) = e^{-isd\hat{p}} \psi_{\alpha}(x_m), \quad (\text{A.5})$$

where $\hat{p} = -i\partial_x$ is the momentum operator. We then finally obtain

$$\begin{aligned} \hat{O} \sum_{\alpha,m} \psi_{\alpha}(x_m) w_{\alpha,m}(x) &= \sum_{\alpha,\beta,m} \sum_s O_{\beta,\alpha}^{(s)} e^{-isd\hat{p}} \psi_{\beta}(x_m) w_{\alpha}(x - x_m) \\ &= \sum_{\alpha,\beta,m} O_{\alpha,\beta}(\hat{p}) \psi_{\beta}(x_m) w_{\alpha,m}(x). \end{aligned} \quad (\text{A.6})$$

Comparing coefficients we find the desired relation

$$\hat{O} \psi_{\alpha}(x) = \sum_{\beta} O_{\alpha,\beta}(\hat{p}) \psi_{\beta}(x). \quad (\text{A.7})$$

-
- [1] I. Bulutaand and F. Nori, Science **326**, 106 (2009).
 - [2] I. Bloch, J. Dalibard, and W. Zwerger, Rev. Mod. Phys. **80**, 885 (2008).
 - [3] L. J. Garay, J. R. Anglin, J. I. Cirac, and P. Zoller, Phys. Rev. Lett. **85**, 4643 (2000).
 - [4] L. Lamata, J. León, T. Schätz, and E. Solano, Phys. Rev. Lett. **98**, 253005 (2007).
 - [5] R. Gerritsma, F. Zähringer, E. Solano, R. Blatt, and C. F. Roos, Nature **463**, 68 (2010).
 - [6] J. Casanova, J. J. Garcia-Ripoll, R. Gerritsma, C. F. Roos, and E. Solano, Phys. Rev. A **82**, 020101 (2010).
 - [7] R. Gerritsma, B. Lanyon, G. Kirchmair, F. Zähringer, C. Hempel, J. Casanova, J. J. Garcia-Ripoll, E. Solano, R. Blatt, and C. F. Roos, Phys. Rev. Lett. **106**, 060503 (2011).
 - [8] G. Juzeliunas, J. Ruseckas, M. Lindberg, L. Santos, and P. Öhberg, Phys. Rev. A **77**, 011802(R) (2008).
 - [9] J. Otterbach, R. G. Unanyan, and M. Fleischhauer, Phys. Rev. Lett. **102**, 063602 (2009).
 - [10] D. Witthaut, Phys. Rev. A **82**, 033602 (2010).
 - [11] J. I. Cirac, P. Maraner, and J. K. Pachos, Phys. Rev. Lett. **105**, 190403 (2010).
 - [12] S.-L. Zhu, B. Wang, and L.-M. Duan, Phys. Rev. Lett. **98**, 260402 (2007).
 - [13] S. Longhi, Phys. Rev. B **81**, 075102 (2010).
 - [14] V. Apaja, M. Hyrkäs, and M. Manninen, Phys. Rev. A **82**, 041402 (2010).
 - [15] G. Ritt, C. Geckeler, T. Salger, G. Cennini, and M. Weitz, Phys. Rev. A **74**, 063622 (2006).
 - [16] T. Salger, C. Geckeler, S. Kling, and M. Weitz, Phys. Rev. Lett. **99**, 190405 (2007).
 - [17] T. Salger, C. Geckeler, S. Kling, and M. Weitz, Science **326**, 1241 (2009).
 - [18] F. Bloch, Z. Phys. **52**, 555 (1928).
 - [19] W. Kohn, Phys. Rev. **115**, 809 (1959).
 - [20] D. Jaksch, C. Bruder, J. I. Cirac, C. W. Gardiner, and P. Zoller, Phys. Rev. Lett. **81**, 3108 (1998).
 - [21] B. Thaller, *The Dirac equation*, Springer, Berlin Heidelberg New York (1992).
 - [22] J. C. Slater, Phys. Rev. **76**, 1592 (1949).
 - [23] J. M. Luttinger, Phys. Rev. **84**, 814 (1951).
 - [24] E. N. Adams II, Phys. Rev. **85**, 41 (1952).
 - [25] G. Sundaram and Q. Niu, Phys. Rev. B **59**, 14915 (1999).